

## **Experimental and numerical determination of relative slips in a contact under fretting conditions**

Martin Nesládek<sup>1</sup>, Jiří Kuželka<sup>2</sup>, Jan Růžička<sup>3</sup>, Josef Jurenka<sup>4</sup> & Miroslav Španiel<sup>5</sup>

**Abstract:** This paper briefly summarizes the current knowledge concerning the fretting phenomenon. Our laboratory equipment for fretting fatigue testing is introduced and the results of preliminary fatigue tests are presented. According to the acquired data and experience, significant modifications of the testing apparatus were performed in order to provide exact and reproducible fretting experiments. The goal of this work is estimation of the contact slips in a contact interface. In the first stage, the contact slips were measured using the digital image correlation method. Subsequently, friction calibration in an FE model is to be performed using the obtained data.

**Keywords:** Fretting, Contact slips, FEM, Digital Image Correlation

### **1. Introduction**

The fretting phenomenon can be defined as a material damage which appears in contacts with relative oscillations of small amplitude. These conditions can cause severe material wear in the surface layers. Furthermore, contact interfaces can substitute the role of classical notches. In an extreme case of high stresses they can accelerate the initiation of fatigue cracks. The stress gradients in the contacts are usually significantly higher than those observed in the vicinity of the classical notches. Mostly due to the nonlinear nature of friction, components of the stress tensor vary non-proportionally in the material points close to the contact interface.

The typical representatives of the machine-part couplings subjected to fretting conditions are turbine blade dovetail joints, spline couplings, rivet joints, railway wheel and axle connections, etc. [1].

Together with the above mentioned influence of stress concentrations on the fretting damage, one can recall another two factors related to it. Namely, the first one is the friction characterizing tribological properties of the contact interface. The second one is the contact slipping where the values of relative slips of the contacting surfaces are widely used for description of the contact regimes under the fretting conditions [2]. Regarding the slip range,

---

<sup>1</sup> Ing. Martin Nesládek; Department of Mechanics Biomechanics and Mechatronics, Faculty of Mechanical Engineering, Czech Technical University in Prague; Technická 4, 166 07 Prague, CZ; e-mail: martin.nesladek@fs.cvut.cz

<sup>2</sup> Ing. Jiří Kuželka; Department of Mechanics Biomechanics and Mechatronics, Faculty of Mechanical Engineering, Czech Technical University in Prague; Technická 4, 166 07 Prague, CZ; e-mail: jiri.kuzelka@fs.cvut.cz

<sup>3</sup> Ing. Jan Růžička; Department of Mechanics Biomechanics and Mechatronics, Faculty of Mechanical Engineering, Czech Technical University in Prague; Technická 4, 166 07 Prague, CZ; e-mail: jan.ruzicka@fs.cvut.cz

<sup>4</sup> Ing. Josef Jurenka; Department of Mechanics Biomechanics and Mechatronics, Faculty of Mechanical Engineering, Czech Technical University in Prague; Technická 4, 166 07 Prague, CZ; e-mail: josef.jurenka@fs.cvut.cz

<sup>5</sup> Doc. Ing. Miroslav Španiel; Department of Mechanics Biomechanics and Mechatronics, Faculty of Mechanical Engineering, Czech Technical University in Prague; Technická 4, 166 07 Prague, CZ; e-mail: miroslav.spaniel@fs.cvut.cz

those regimes are: the stick regime with the slip magnitude up to  $3\text{ }\mu\text{m}$ , the partial slip regime with the slips between  $3$  to  $50\text{ }\mu\text{m}$ , and the gross sliding where the slips are more than  $50\text{ }\mu\text{m}$ .

It should be noted that the relation between the slip magnitudes and the fatigue life is not monotonic. One can observe a dramatic decrease in the partial slip regime. This state is specific for sticking in the centre of the interface and for slipping of both surfaces around the contact edges – see Fig. 1. This is the area of the most severe material damage which can together with high stresses act as “the weakest link” accelerating fatigue crack nucleation.

The decrease of the fatigue life in the partial-slip regime is followed by a rapid increase in the phase of transition to the gross sliding. This is due to a more intensive material erosion which removes crack nucleuses.

All the three above mentioned factors – stress, friction and contact slips – are closely dependent and in the real structures they change during their life-time.

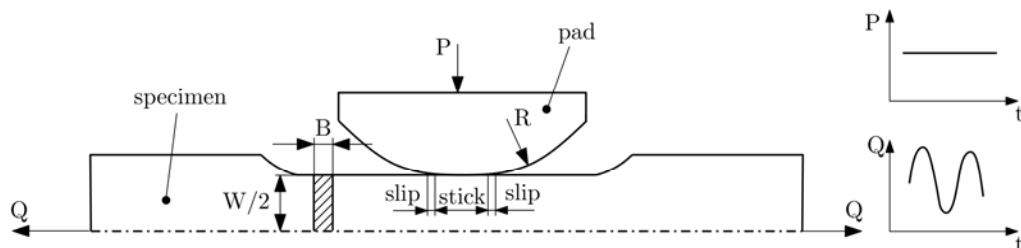


**Fig. 1.** A typical laboratory configuration for simulation of partial-slip fretting conditions (cylinder on a flat contact geometry). The same concept was adopted in our experiments

### 1.1. Damage estimations under fretting conditions

Due to the multiaxial stress state in the fretted contact, conventional multiaxial fatigue criteria based on the critical plane estimation are widely used to predict the place of the initiation and the direction of the initial crack growth. Relations for conversion of some of these criteria to the number of cycles can be found e.g. in [3].

In the last decade, some authors have been trying to adopt the simulation procedure including surface wear based on the Archard's formula [4] or the dissipated energy concept [5]. Nevertheless, incremental estimation of wear together with damage cumulation is still unfeasible for real structures.

Another possibility how to improve the results of conventional fatigue criteria is to incorporate certain correction with respect to the fretting wear. Ideally, it should reflect the values that cause surface damage, i.e. relative slips and surface shear stress. Ding et al. [6] introduced a simple parameter  $D_{fret2}$  correcting the multiaxial SWT criterion. According to the authors, the main contribution of  $D_{fret2}$  is that SWT can now handle the increase in the fatigue life in the transition domain between the partial and gross slips.

The goal of the presented work is to verify specific multiaxial fatigue criteria by the fatigue tests. New testing equipment was developed for this purpose and a digital image correlation method was newly employed in this field in order to calibrate the FE model.

## 2. Original equipment for fatigue experiments under fretting conditions

In [7] the concept of the new equipment for testing of fatigue under fretting conditions at the Faculty of Mechanical Engineering of the Czech Technical University in Prague, developed in the scope of an acknowledged project, was briefly introduced. It is designed for a single dog-bone specimen in contact with two cylindrical fretting pads. The main advantage of the

cylinder on a flat contact geometry is the simplicity of the partial-slip regime accomplishment. Another benefit of the proposed setup is the possibility of its use in standard fatigue testing machines. The present state of the equipment prepared for the experiment is shown in Fig. 2.

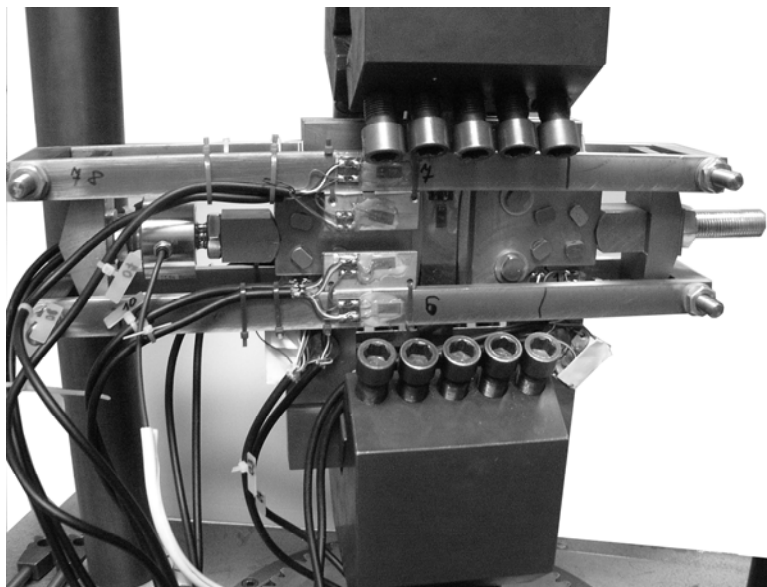


**Fig. 2.** The setup for the fretting fatigue testing. The equipment is clamped in the jaws of electromagnetic pulsator AMSLER

The specimen is vertically clamped in the jaws of the testing machine and axially loaded by a time-varying force which is set by the machine control system. The loading frequency corresponds to the natural frequency of the system which reflects the mass of the machine and the stiffness of additional experimental equipment and the specimen. The normal contact force acts in the horizontal direction which is perpendicular to the axial cyclic loading. This force is kept constant during a single test. Values of the contact force can be monitored in real time by the dynamometer.

Each specimen is equipped by strain gauges for measuring of the auxiliary bending which is an undesirable effect. Bending can primarily result from inaccurate installation of the testing specimen. Indirect measurement of the friction forces in both contact interfaces is also possible.

### *2.1. Preliminary fatigue tests*

Several experiments were performed in order to verify the quality of the proposed design with respect to the feasibility of exact and reproducible fretting conditions. Geometry of the contact area was monitored with the aim of tuning some possible inaccuracies in the contact surface match.

The loading conditions of the three fatigue experiments that have been carried out so far are provided in Table 1. Numbers of cycles to crack initiation  $N$  are also shown. They were estimated based on the stiffness decrease in the experimental setup. The axial loading frequency was about 100 Hz. The material of the specimens was Cr-Ni-Mo-V martensitic steel with the plain fatigue strength in reversed tension  $f_1 = 485$  MPa. The cross-sectional dimensions were  $B = 6$  mm and  $W = 20$  mm (see Fig. 1). Fretting pads with the radius  $R = 200$  mm were used.

Relatively high scatter can be observed from these data. Especially the difference between tests no. 1 and 3 reflects certain auxiliary influence.

**Table 1. Loading conditions and number of cycles to crack initiation in the fretting experiments**

| Experiment no. | $Q_{amp.}$ [N] | $Q_{mean}$ [N] | P [N] | N [-]     |
|----------------|----------------|----------------|-------|-----------|
| 1              | 14             | 15             | 15    | 2 849 000 |
| 2              | 14             | 15             | 5     | 1 577 000 |
| 3              | 14             | 15             | 15    | 1 676 000 |

Relief of both contact surfaces of each specimen was scanned by a digital microscopic camera with 2Mpix resolution. Panoramic pictures, like those in Fig. 3 and Fig. 4, were then obtained by merging more than 100 single scans.

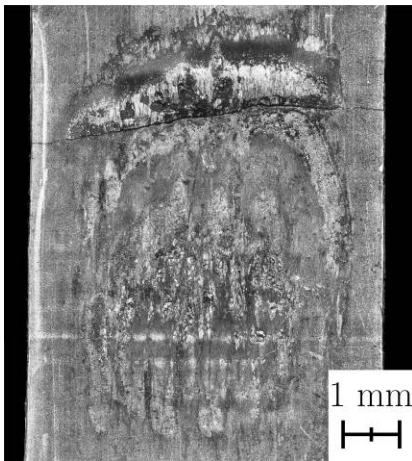


**Fig. 3.** Detail of worn contact surface of the specimen after fretting test no. 1 – side A

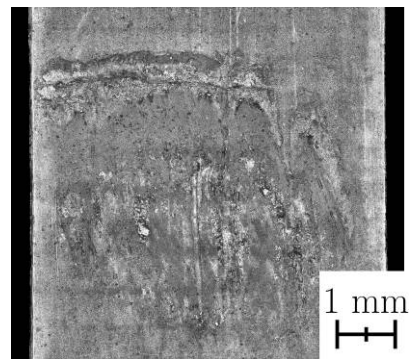


**Fig. 4.** Detail of worn contact surface of the specimen after fretting test no. 1 – side B

Fatigue crack initiation always took place on the top contact edge – see Fig. 3 and Fig. 4 which are vertically oriented according to the position of the specimen in the testing rig (Fig. 2). This fact is in line with the general assumptions that the crack initiation usually occurs in the slipping area of a contact in the partial-slip regime. This is also the place of the most severe damage of the exterior faces as can be observed from the pictures of the surface relief. By contrast, mild damage of the central contact area where sticking occurs can be seen.

Contact loading was concentrated mostly in the centre of the specimens and fretting pads. In some cases, the contact area was shifted from the centre towards the edge of the specimen. This violates the assumption about the uniform load distribution between both specimen edges that was also proved by the FE models.

## 2.2. Modifications of experimental equipment

Regarding the above observations of improper contact loading distribution, revision of the testing apparatus was done in order to reveal sources of this problem. Severe inaccuracy in the surface finish of the fretting pads was detected by roughness tester. In the transverse direction, the measured surface contour was curved instead of being straight. To circumvent this problem, a more precise finishing was performed on a CNC machine.

Another design modification was done on the fretting pad bearing surfaces – see Fig. 5 and Fig. 6. A detail of the pad installation in the testing apparatus is shown in Fig. 7. Rigidity

of the original alternative did not allow rotation of the fretting pads which could eliminate the initial non-parallel setup of the contact surfaces. That is the reason why additional chamfers were manufactured. Together with lateral gaps as shown in Fig. 6, this arrangement is capable of compensating the initial inaccuracies given by manufacturing.

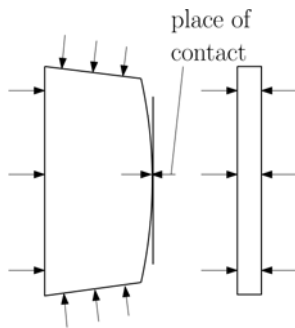


**Fig. 5.** The original fretting pad geometry with flat side faces. The arrows show where the pad was connected to the rest of the structure

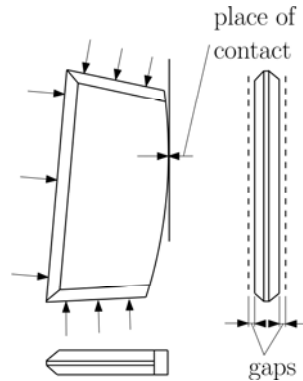


**Fig. 6.** The modified fretting pad geometry with additional chamfers and lateral gaps allowing better match with the contact surface of a specimen. The rotated position enables a one-off reuse of the same pad



**Fig. 7.** Detail of the fretting pad installation in the experimental equipment – the original configuration without chamfers

Usually no fatigue cracks occur on the pads after the experiment termination. The contact surfaces can then be renovated by grinding and after that the pads can be reused. Since this is a costly operation, the following simple modification of the fretting pad installation was introduced. Both pads are now fixed in a moderately rotated position (compare Fig. 5 and Fig. 6). Due to this, the contact area is shifted horizontally on the fretting pads which enables their one-off reuse when they are installed upside down. The beneficial effect is that it will halve the time losses and expenses for their renovation.

### 3. Experimental and numerical estimation of contact slips

#### 3.1. Arrangement of the experiment

The optical system Dantec Dynamics Q-450 based on the digital correlation method was used for the experimental estimation of the contact slips, i.e. the relative contact displacement of the specimen and fretting pad. Due to the displacements in the order of  $\mu\text{m}$  and high frame rates,

high demands were laid on the surface speckle pattern and lighting. Regarding the 1 Mpix resolution of the CCD chip, the objective and extension tubes were used to achieve spatial resolution of 8  $\mu\text{m}/\text{pix}$ . The viewed surfaces were coated by a fine contrast stochastic speckle pattern created by an airbrush considering the recommendations in [8]. Two special high frequency lamps with 1 kW power each were used for lighting. The images of the vicinity of the contact interface were recorded by a high speed camera with the frequency of 2 kHz (corresponds to 20 images per loading cycle).

The data presented below were measured on the experimental setup (see Fig. 2) with design modifications explained in the previous section.

### 3.2. Measured data processing

The acquired sets of image sequences were processed in the commercial image correlation software Istra 4-D. The displacements were evaluated in a 0.1 mm (12 pix) equally spaced grid. Each grid point corresponds to a subset 0.2x0.2 mm (25x25 pix). The obtained results were further post-processed by Matlab scripts.

The point with maximal contact pressure (and thus the centre of the contact area) was estimated on the basis of displacement field in case of pure pressure loading of 10 kN magnitude. At this point, a coordinate system for relative slip evaluation was introduced. The Hertz contact theory was applied for the estimation of the contact area width.

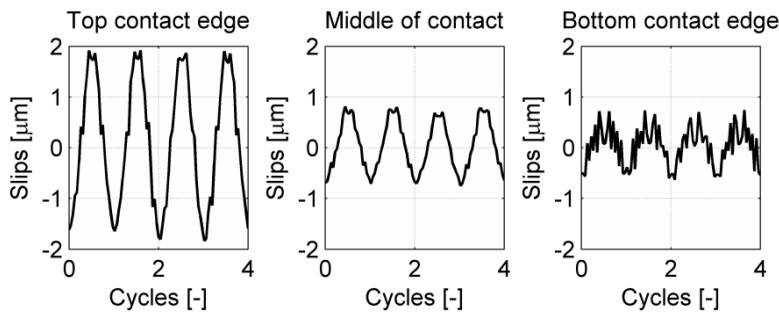


**Fig. 8.** Experimentally measured time history of relative slips in different locations in the contact interface for 5 kN pressure loading. Orientation of the contact edges corresponds to the configuration in Fig. 9

The relative slips were computed as a difference between the displacements along a line near the contact edge on the specimen and the pad. The time behaviour of the contact slips on the top, in the middle and on the bottom of the contact area is shown in Fig. 8. The changing character of slipping from the more loaded side (top) to the less loaded side (bottom) can be observed.

### 3.3. FE model

To obtain detail input data for the fatigue criteria, a 3D FE model of the testing apparatus was assembled – see Fig. 9 – and analysed. The commercial solver Abaqus/Standard was used for the numerical simulation which was divided into several computation steps reflecting pressure and axial preload and application of axial cyclic loading. The material model was assumed to be liner-elastic. The geometry was discretised by linear hexahedral continuum elements. The smallest element edge in the contact area was 85  $\mu\text{m}$  – see Fig. 10 and Fig. 11.

A proper model of the contact friction has a significant effect on reliability of the fretting analysis results. The friction coefficient used in the fretting simulations is usually higher than in a conventional contact and should reflect its change during the life-time. Abaqus contact algorithms adopt several computation techniques. In our model, surface-to-

surface discretisation, finite-sliding tracking approach and hard contact with the Coulomb friction was applied. The friction coefficient was set to 0.8 and was enforced by the method of Lagrange multipliers.

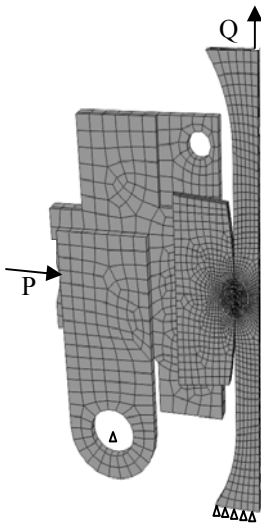


**Fig. 9.** Global view of the 3D FE model of the testing apparatus

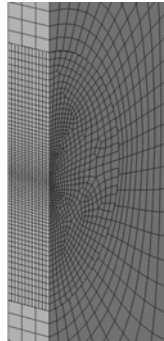


**Fig. 10.** Detail of the specimen mesh

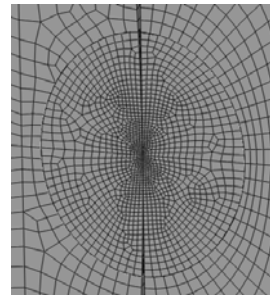


**Fig. 11.** View of the contact area mesh (the specimen is on the right)

### 3.4. Comparison of numerical and experimental results

At first, a proper quantity for comparison of the experimental and numerical results must be determined. The choice of the slip amplitudes along the contact area could be misleading for this purpose. According to the experimental results, this quantity is not convenient since approaching the bottom edge of the contact the slipping process becomes more stochastic. Moreover, the amplitudes in the middle of the contact are as high as on the bottom – see Fig. 8.

When using a more integral quantity a better conformity can be expected. Accumulated slips per single period appear to be a more suitable measure. This quantity has a clearer physical meaning than the slip amplitudes and can be used for a steady-state results comparison as is shown in Fig. 12. Three loading regimes according to the contact pressure force 5, 10 and 15 kN are compared here.

## 4. Conclusions

The presented results of the fatigue experiments under fretting conditions revealed improper distribution of the contact loads. Consequently, several modifications in the equipment design were performed. These are mostly related to geometry and installation of the fretting pads. Subsequent tests proved that the new design has the capability to distribute the contact loads over the whole specimen width as was originally expected. This should result in a reduced scatter in the fatigue experiments.

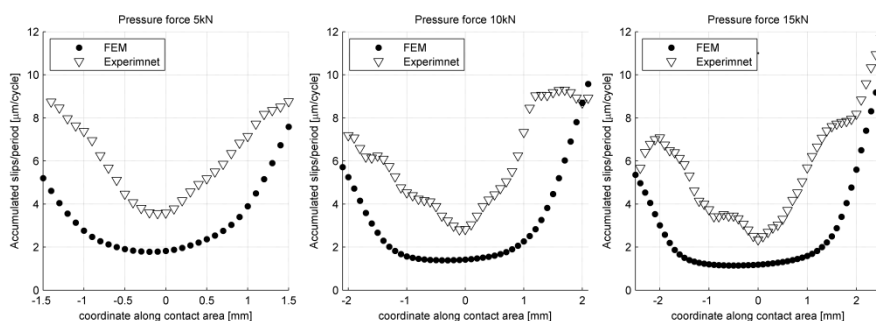


**Fig. 12.** Accumulated relative slips per single cycle period along the contact interface for 5, 10 and 15 kN pressure force

On this tuned experimental setup several measurements were performed in order to acquire reliable values of the contact slips for further FE model calibration. As can be seen from the time history of the relative contact slips, this quantity has a changing character with respect to the position along the contact. This behaviour cannot be simulated by a relatively cheap steady-state numerical solution. An explicit dynamic formulation of the problem might give a better correlation of this quantity which is a further goal of this project.

By varying the parameters of the numerical model (especially friction) a better correlation can be expected between the numerical and experimental data. In this case the Coulomb friction with the coefficient 0.8 was used. It reflects the average tribological conditions in the contact. By contrast, the experimental data were measured in the beginning of the cyclic loading. This could be an explanation for the observed shift in Fig. 12.

## Acknowledgement

This project was supported by GAČR grant no. 101/09/1709.

## References

- [1] Hoepfner, D.W., Fretting fatigue case studies of engineering components, *Tribology Int.*, 39, pp. 1271-1276 (2006).
- [2] Vingsbo O., Soderberg, S., On fretting wears, *Wear*, 126, pp. 131-147 (1988).
- [3] Navarro, C., Muñoz, S., Domínguez, J., On the use of multiaxial fatigue criteria for fretting fatigue life assesment, *Int. J. of Fatigue*, 30, pp. 32-44 (2008).
- [4] Madge, J.J., Leen, S.B., McColl, I.R., Shipway, P.H., Contact-evolution based prediction of fretting fatigue life: Effect of slip amplitude, *Wear*, 262, pp. 1159-1170 (2007).
- [5] Mary, C., Fouvry, S., Numerical prediction of fretting contact durability using energy wear approach: Optimisation of finite-element model, *Wear*, 263, pp. 444-450 (2007).
- [6] Ding, J., Houghton, D., Williams, E.J., Leen, S.B., Simple parameters to predict effect of surface damage on fretting fatigue, *Int. J. of Fatigue*, 33, pp. 332-342 (2011).
- [7] Kuželka, J., Chlup, H., Jurenka, J., Španiel, M., Fatigue degradation in the vicinity of contact interface under fretting conditions, in *Proceedings of Experimental Stress Analysis*, Velké Losiny, Czech Rep., June 2010, pp. 201-208. ISBN 978-80-244-2533-7.
- [8] Sutton A.M., Orteu J. and Schreier W.H., *Image Correlation for Shape, Motion and Deformation Measurements* (Springer, New York, 2009). ISBN 978-0-387-78746-6.